Supplementary information

Manuscript ID: **NJ-ART-10-2025-004085**

Article type: **Revised Manuscript**

Submitted to: **New Journal of Chemistry**

Copper(II) Complexes of Dipica and Its Derivatives as Biomimetic Models for Phenoxazinone Synthase: Probing the Effect of Central *N*-cycloalkyl Rings on Reactivity

Ganesh Yamuna,[1] Devaraj Karthickram,[1] Narasimman Palani,[1] Nattamai Bhuvanesh[2] and Karuppasamy Sundaravel[1*]

[1]Bioinorganic Research Laboratory, Department of Chemistry, Bharathiar University, Coimbatore – 641 046, Tamil Nadu, India.

[2]X-ray Diffraction Laboratory, Texas A&M University, College Station, TX 77842, United States. Email: nbhuv@chem.tamu.edu

*Author to whom correspondence should be addressed: Email: sundaravel.k@buc.edu.in
sundaravel.k@gmail.com
Tel: +91-422-2428318

Table of Contents

1. Supplementary figures		
Figure S1–S4	^{1}H and ^{13}C NMR spectra of ligands **L1**–**L4** in $CDCl_3$	S1–S5
Figure S5 & S6	ESI-MS profile of ligands **L1**–**L4**	S6 & S7
Figure S7	ATR-IR of ligands **L1**–**L4** and complexes **1**–**4**	S8
Figure S8 & S9	TG-DSC curves of complexes **1**–**4**	S9 & S10
Figure S10 & S11	ESI-MS profile of complexes **1**–**4**	S11 & S12
Figure S12	UV-vis spectral data of complexes **1**–**4**	S13
Figure S13	Cyclic voltammogram of copper(II) complexes **1**, **3** and **4** and their o-aminophenol adducts	S14
Figure S14 & S15	UV-vis spectral changes observed for the oxidation of *o*-aminophenol catalysed by **1**, **3** and **4** in water	S15 & S16
Figure S16–S19	ESI-MS profile of 1:50 mixture of **1**–**4** and H_2AP in methanol-water mixture.	S17–S21
Figure S20	Detection of H_2O_2 by the formation of I_3^- the course of catalytic reaction of **1**–**4** with H_2AP	S22
Figure S21	^{1}H NMR spectrum and ESI-MS profile of phenoxazinone chromophore	S23
Figure S22	UV-vis spectral changes observed for the oxidation of *o*-aminophenol catalysed by **2** in presence of O_2 and N_2 atmosphere in water	S24
2. Supplementary tables		
Table S1	ATR-IR spectral data of ligands **L1–L4** and complexes **1–4**.	S25
Table S2	TG-DSC data of complexes **1–4**.	S26

Figure S1

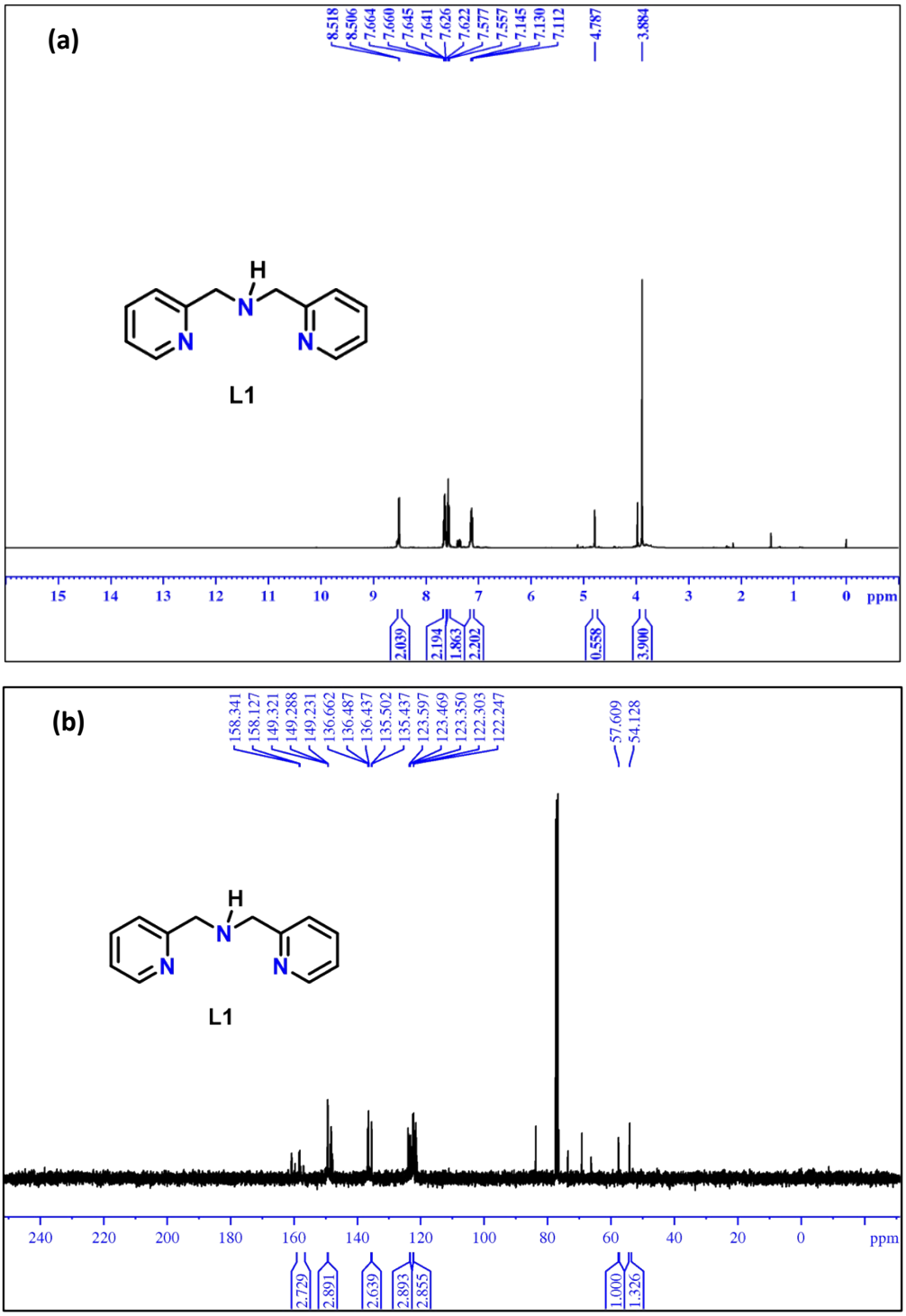

Figure S1. (a) ^{1}H and (b) $^{13}C\{^{1}H\}$ NMR spectra of **L1** in $CDCl_3$ at 298 K.

Figure S2

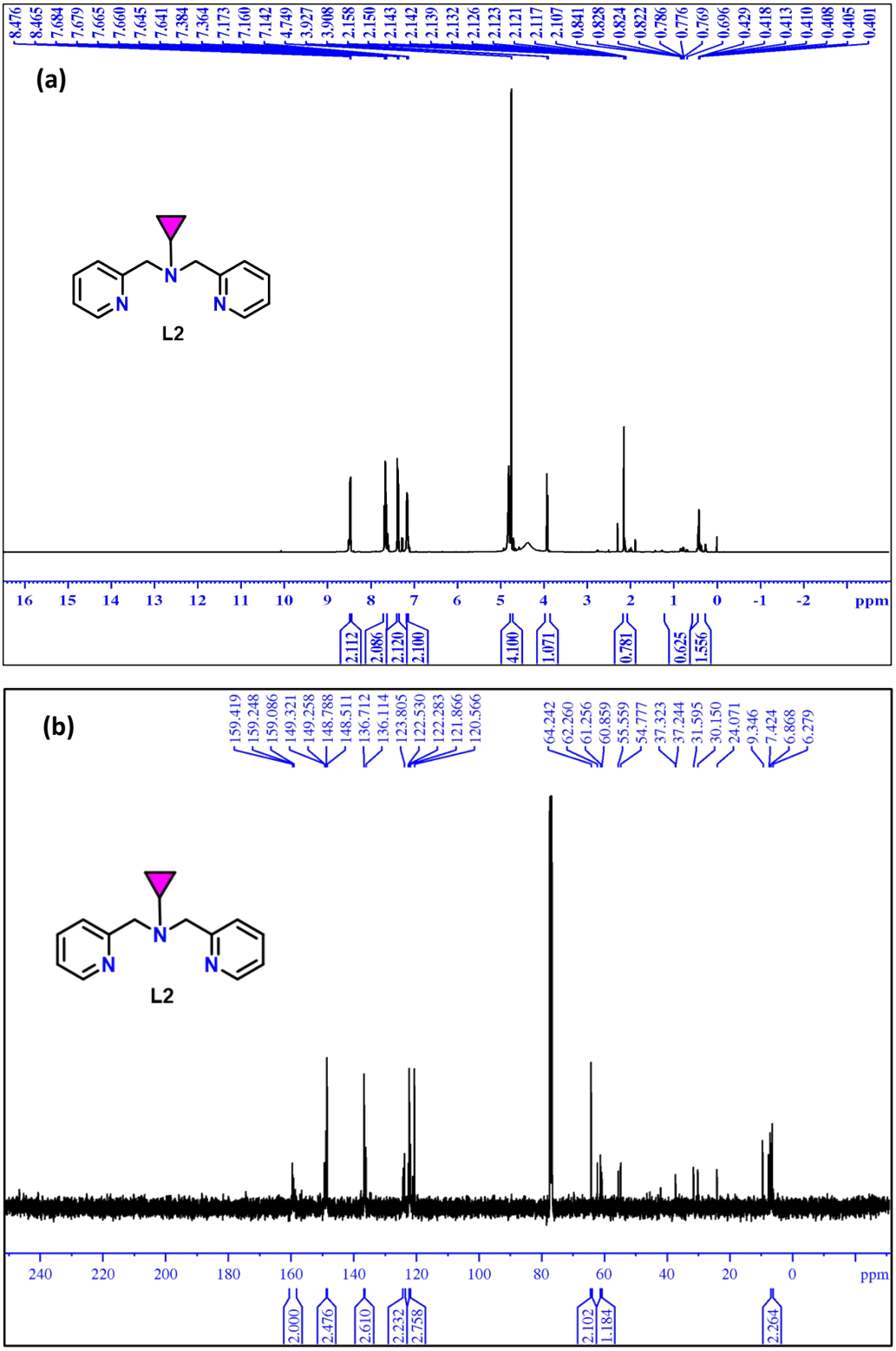

Figure S2. (a) ^{1}H and (b) $^{13}C\{^{1}H\}$ NMR spectra of **L2** in $CDCl_3$ at 298 K.

Figure S3

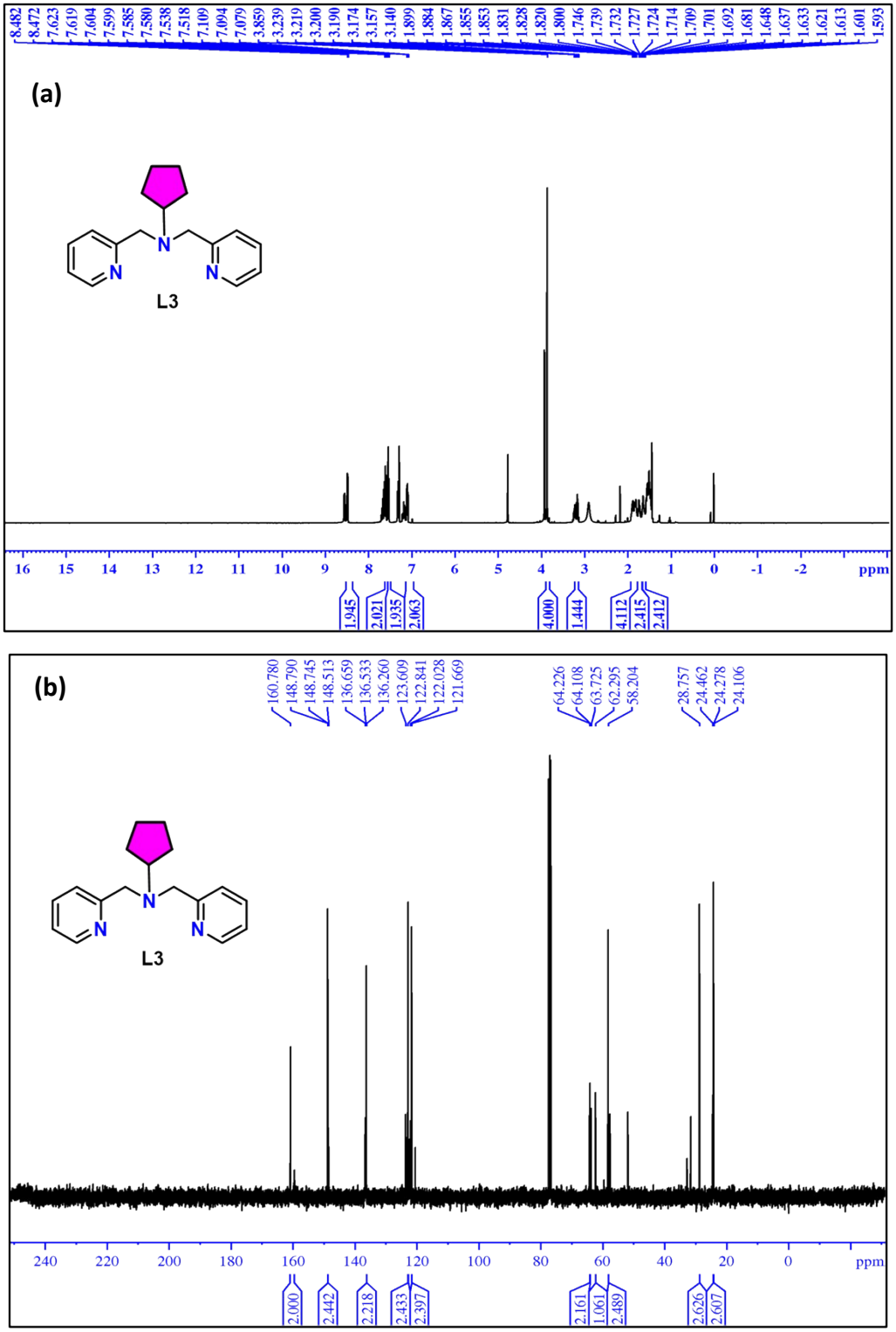

Figure S3. (a) ^{1}H and (b) $^{13}C\{^{1}H\}$ NMR spectra of **L3** in $CDCl_3$ at 298 K.

Figure S4

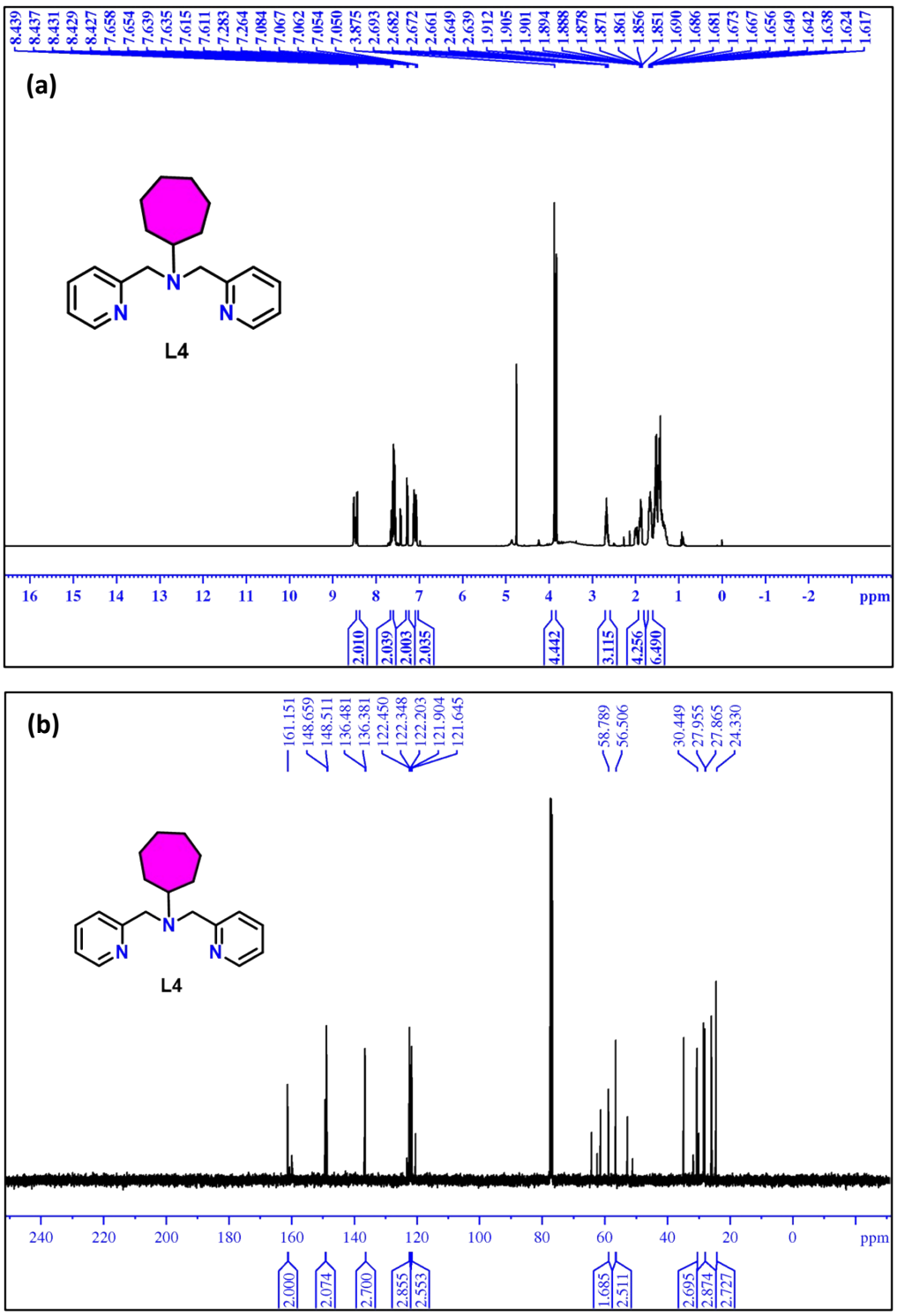

Figure S4. (a) ^{1}H and (b) $^{13}C\{^{1}H\}$ NMR spectra of **L4** in $CDCl_3$ at 298 K.

Figure S5

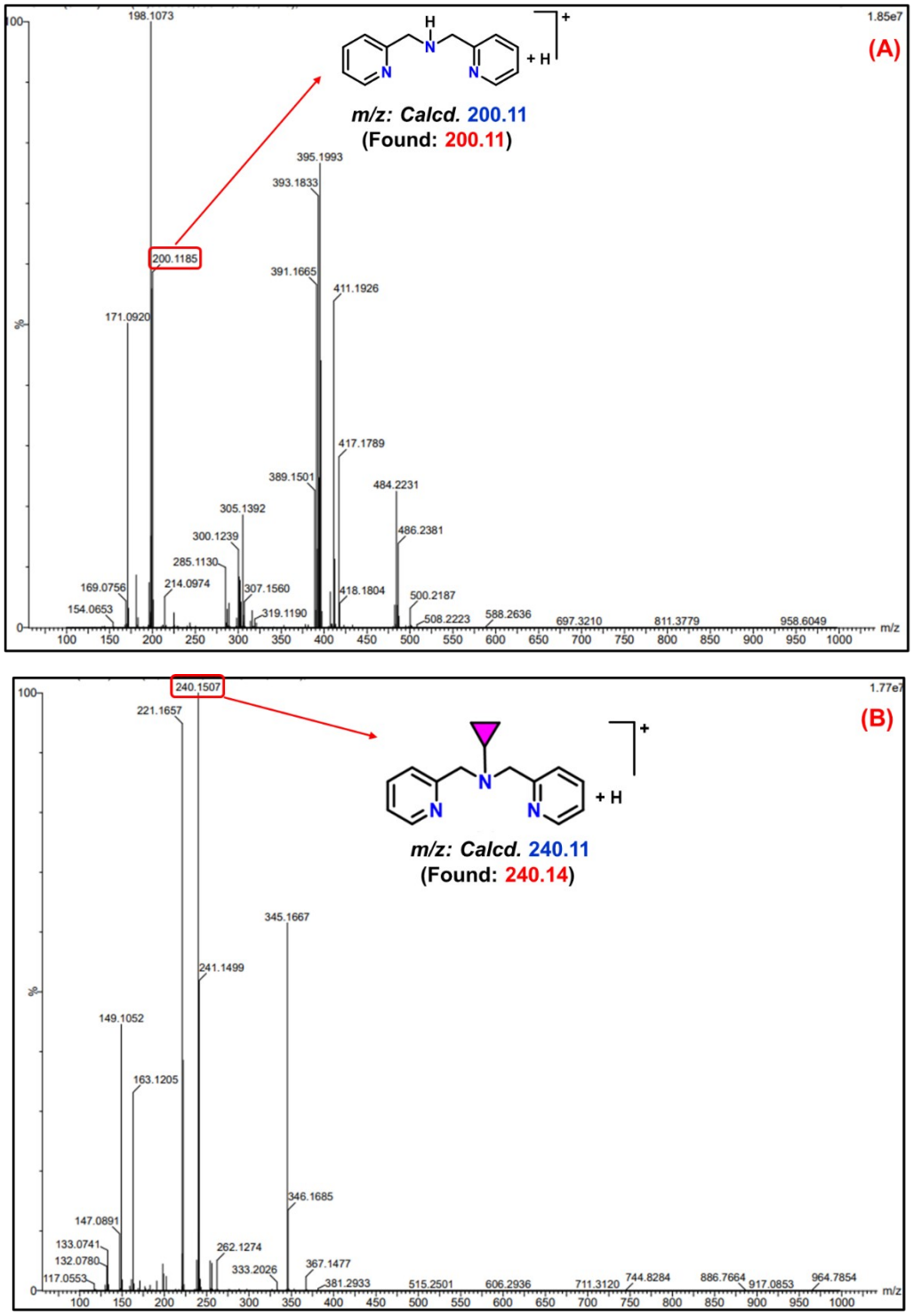

Figure S5. ESI-MS profile of ligands **L1** (A) and **L2** (B) in CH_3OH.

Figure S6

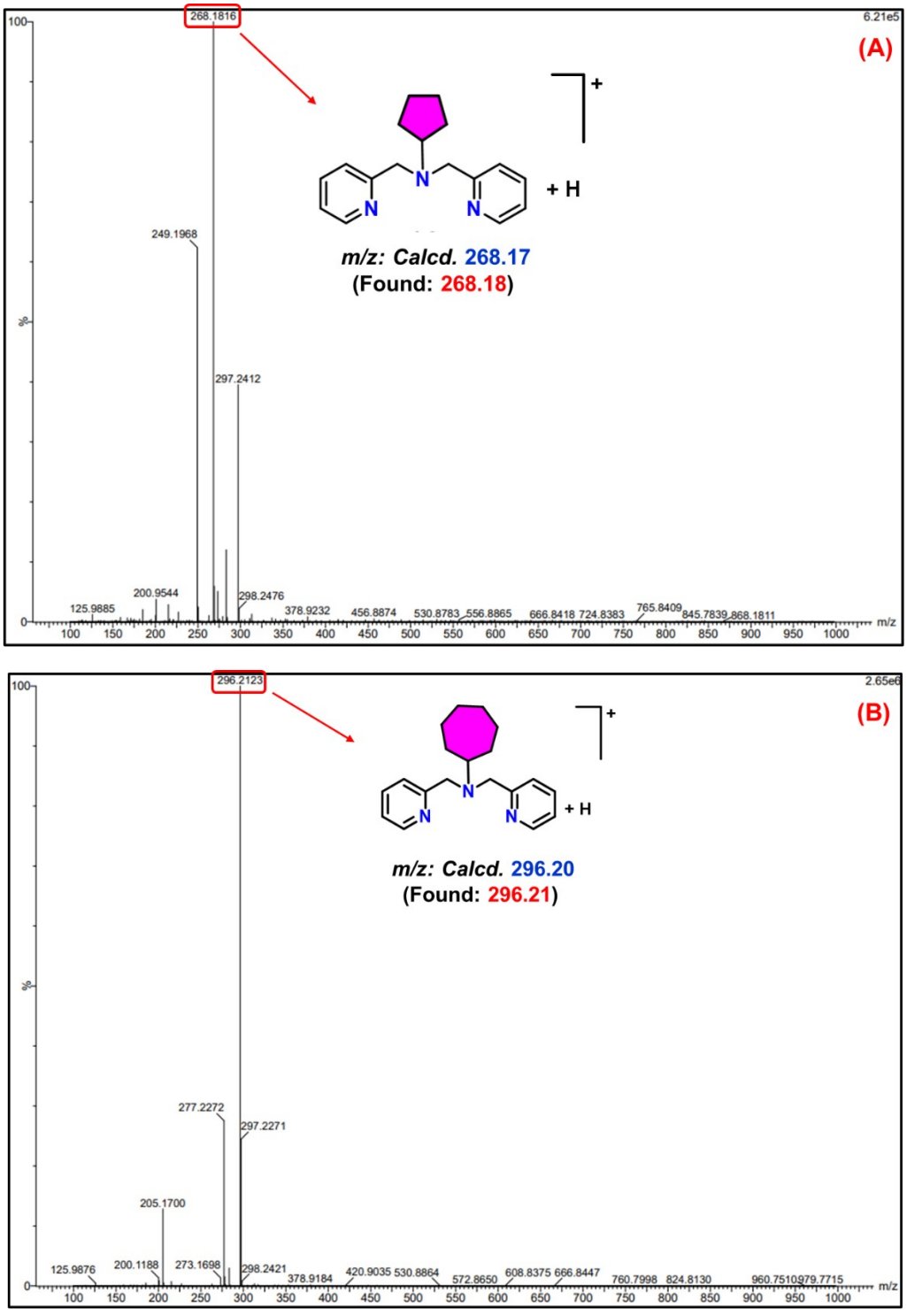

Figure S6. ESI-MS profile of ligands **L3** (A) and **L4** (B) in CH_3OH.

Figure S7

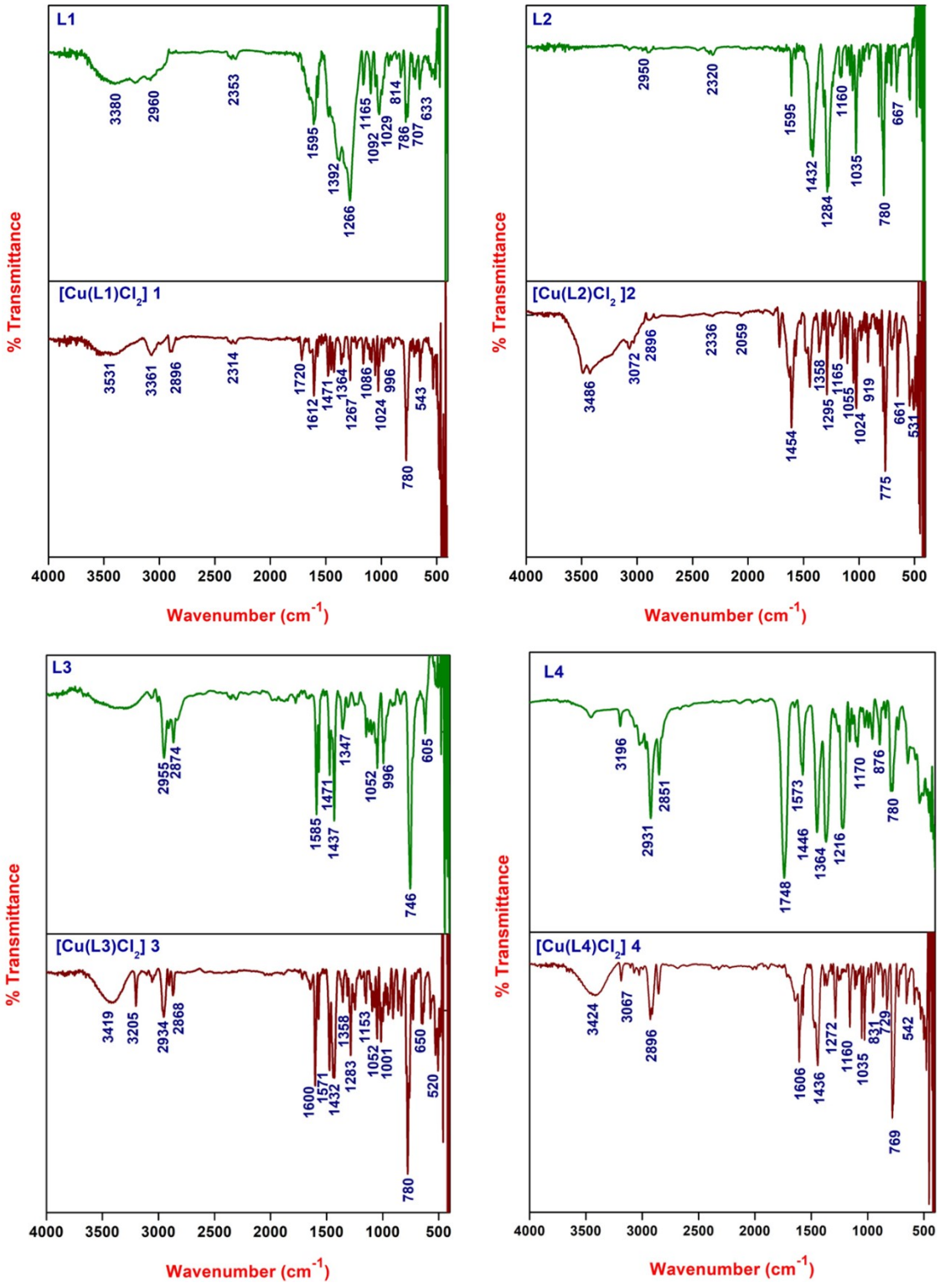

Figure S7. ATR-IR spectral data of ligands **L1**–**L4** and their corresponding complexes **1**–**4**.

Figure S8

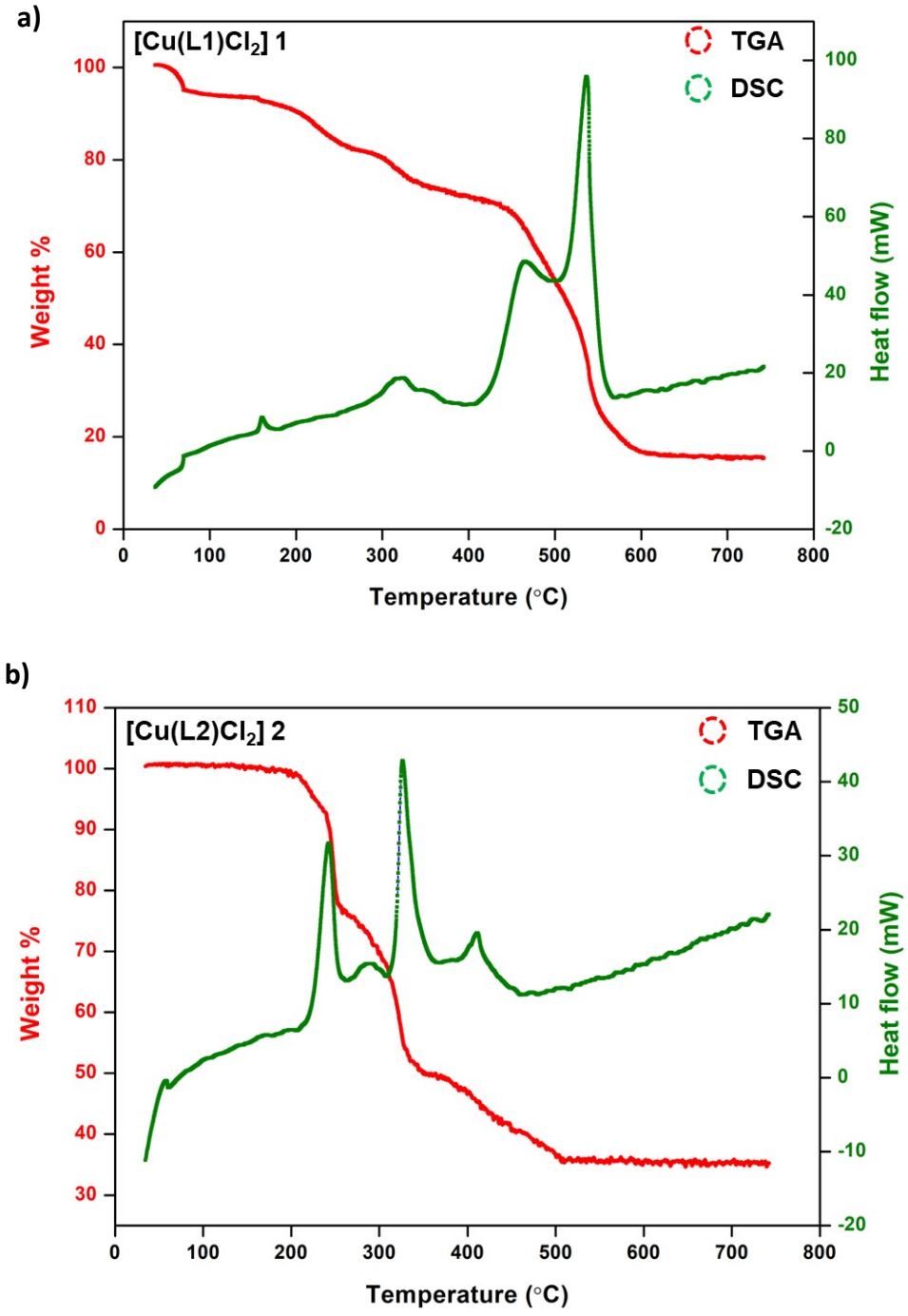

Figure S8. TG-DSC curves of copper(II) complexes **1** (a) and **2** (b).

Figure S9

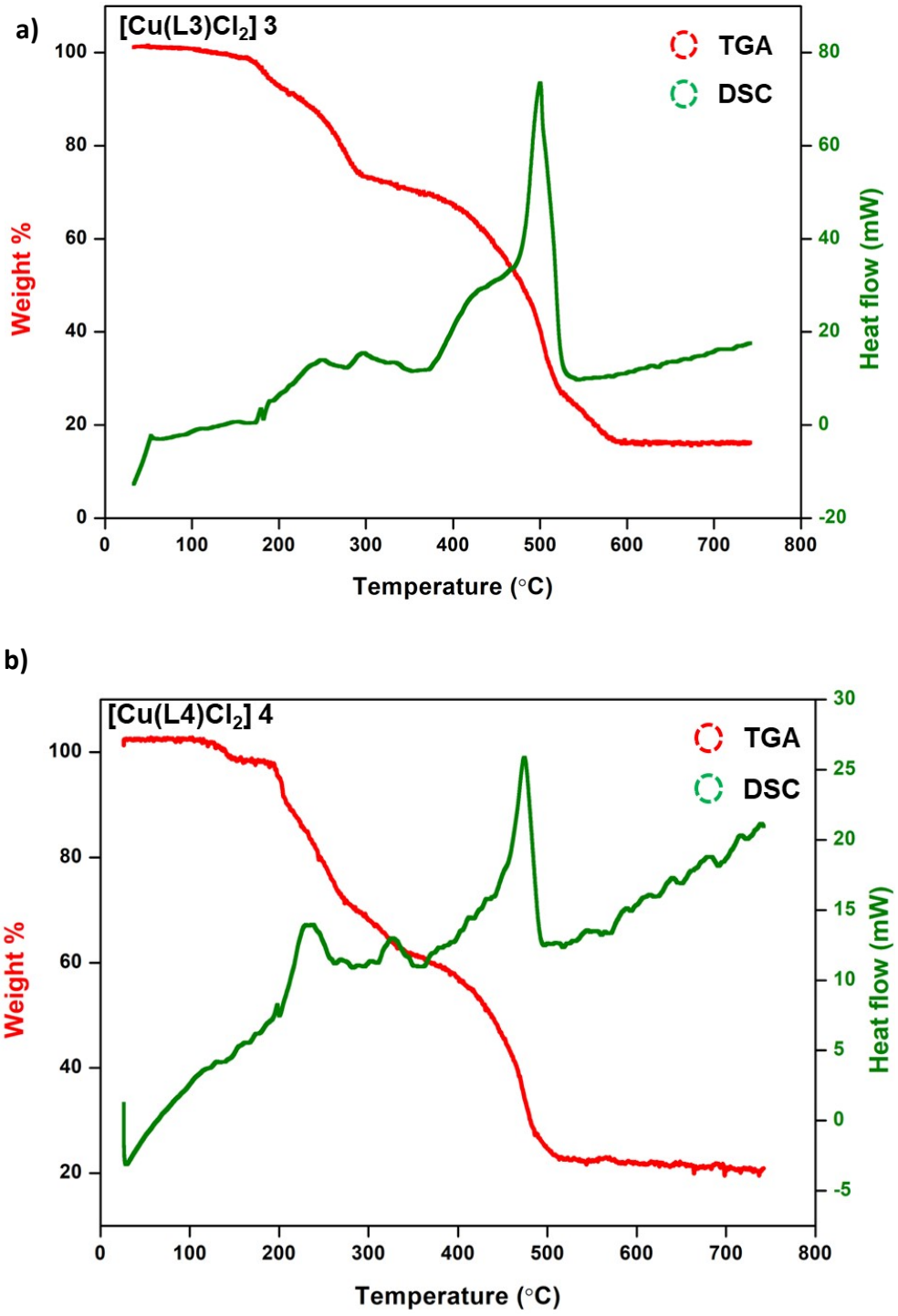

Figure S9. TG-DSC curves of copper(II) complexes **3** (a) and **4** (b).

Figure S10

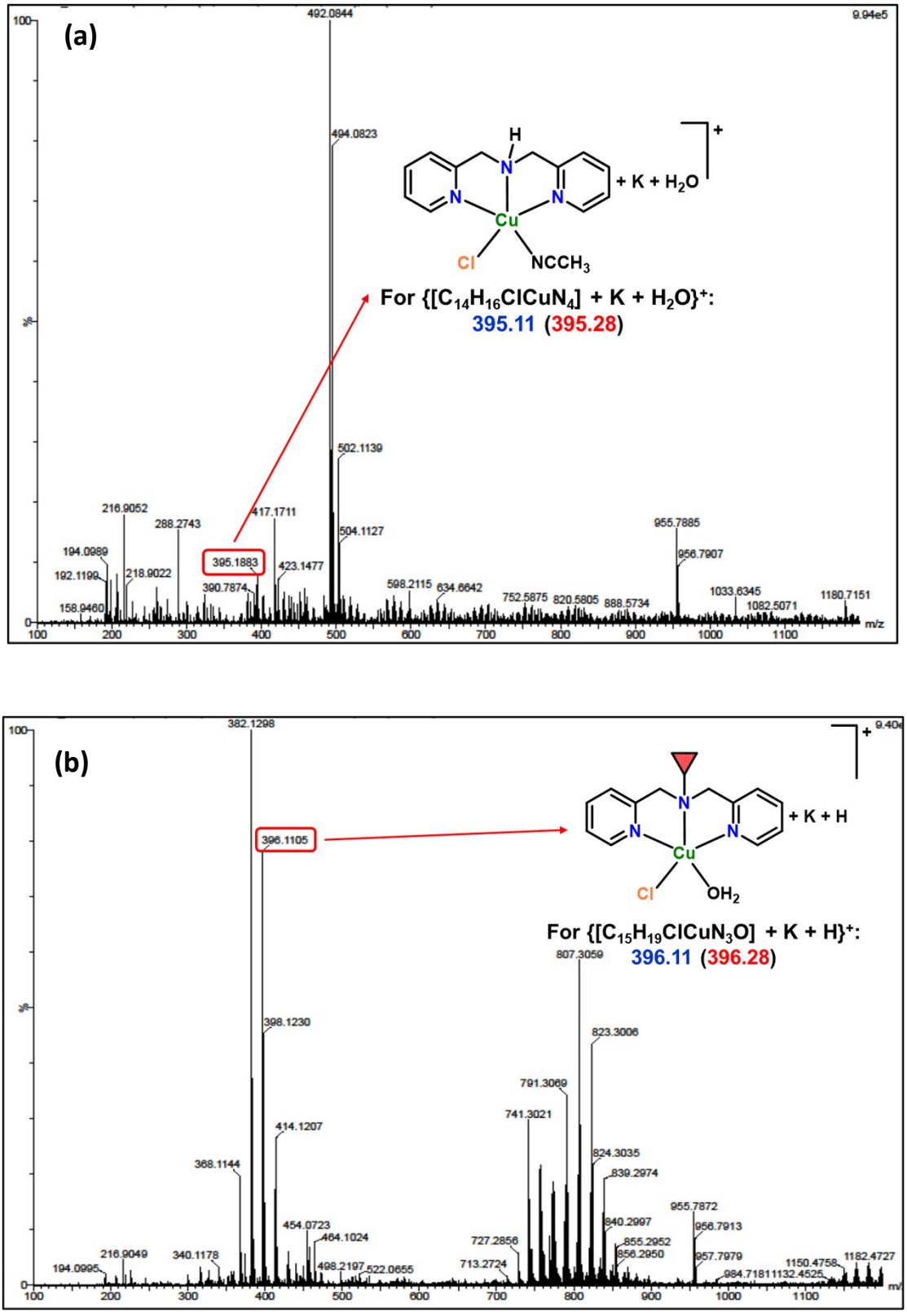

Figure S10. ESI-MS profile of copper(II) complex **1** (a) and **2** (b) in CH_3OH:CH_3CN (1:1 v/v).

Figure S11

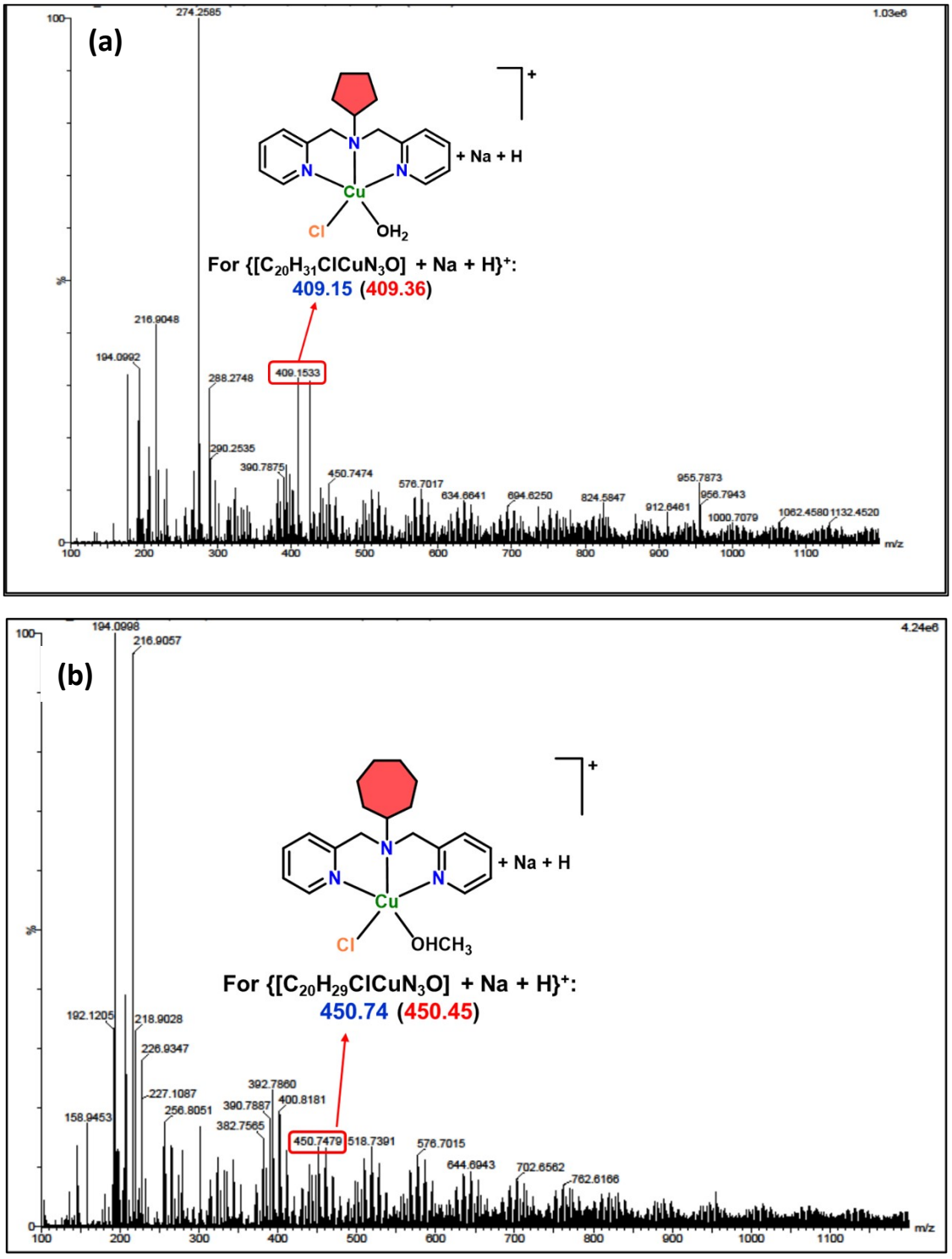

Figure S11. ESI-MS profile of copper(II) complex **3** (a) and **4** (b) in CH_3OH:CH_3CN (1:1 v/v).

Figure S12

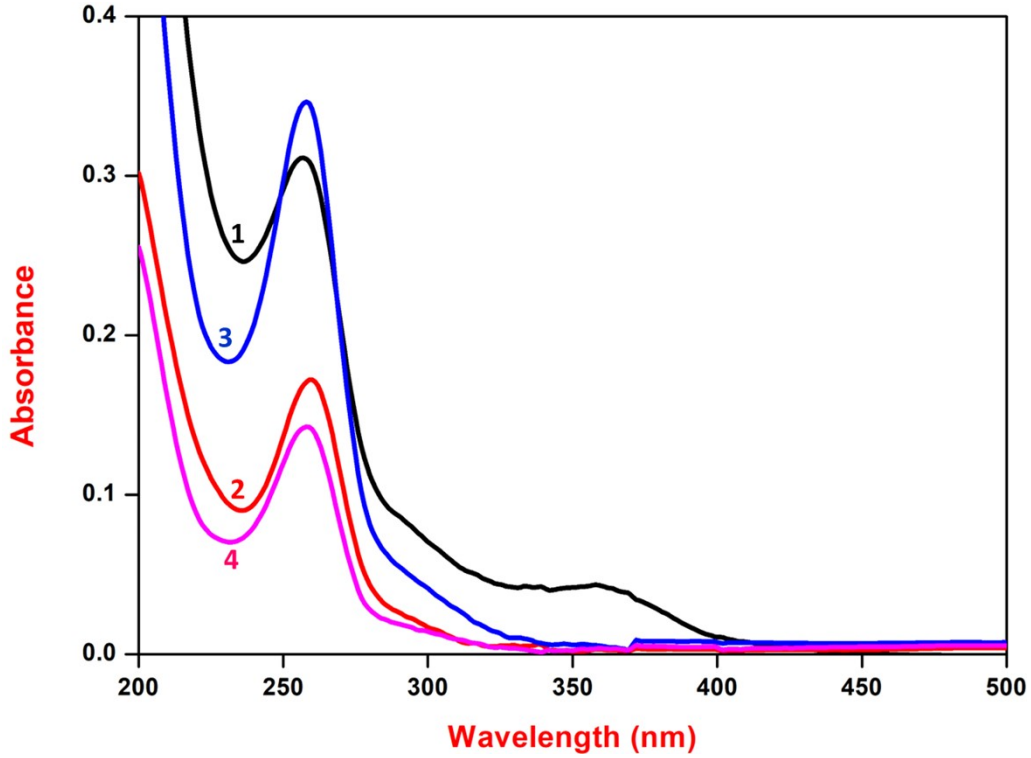

Figure S12. UV-vis absorption spectral data of copper(II) complexes **1** (black) **2** (red), **3** (blue) and **4** (pink) (1×10^{-3} M) in H_2O at 25 °C.

Figure S13

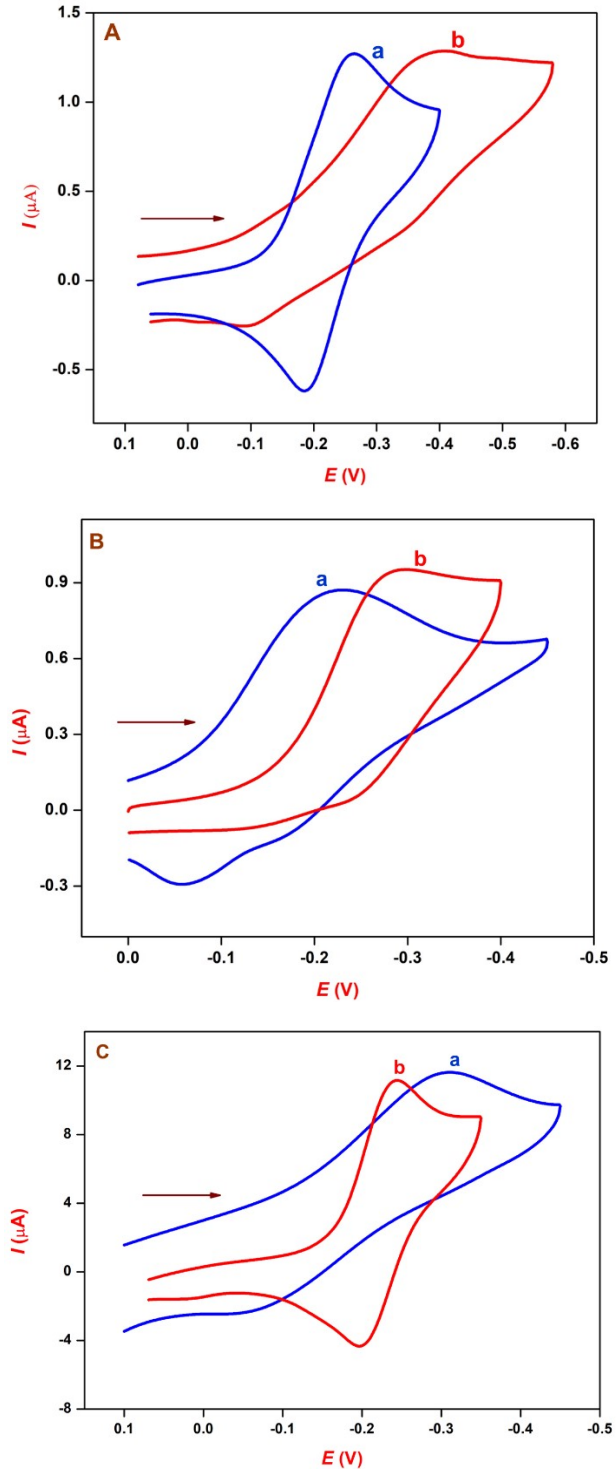

Figure S13. Cyclic voltammogram of **1** (A), **3** (B) and **4** (C) (1×10^{-3} M) in water at 25 °C measured vs saturated Ag/AgCl. Scan rate 50 mV s^{-1} and supporting electrolyte KCl (0.1 M).

Figure S14

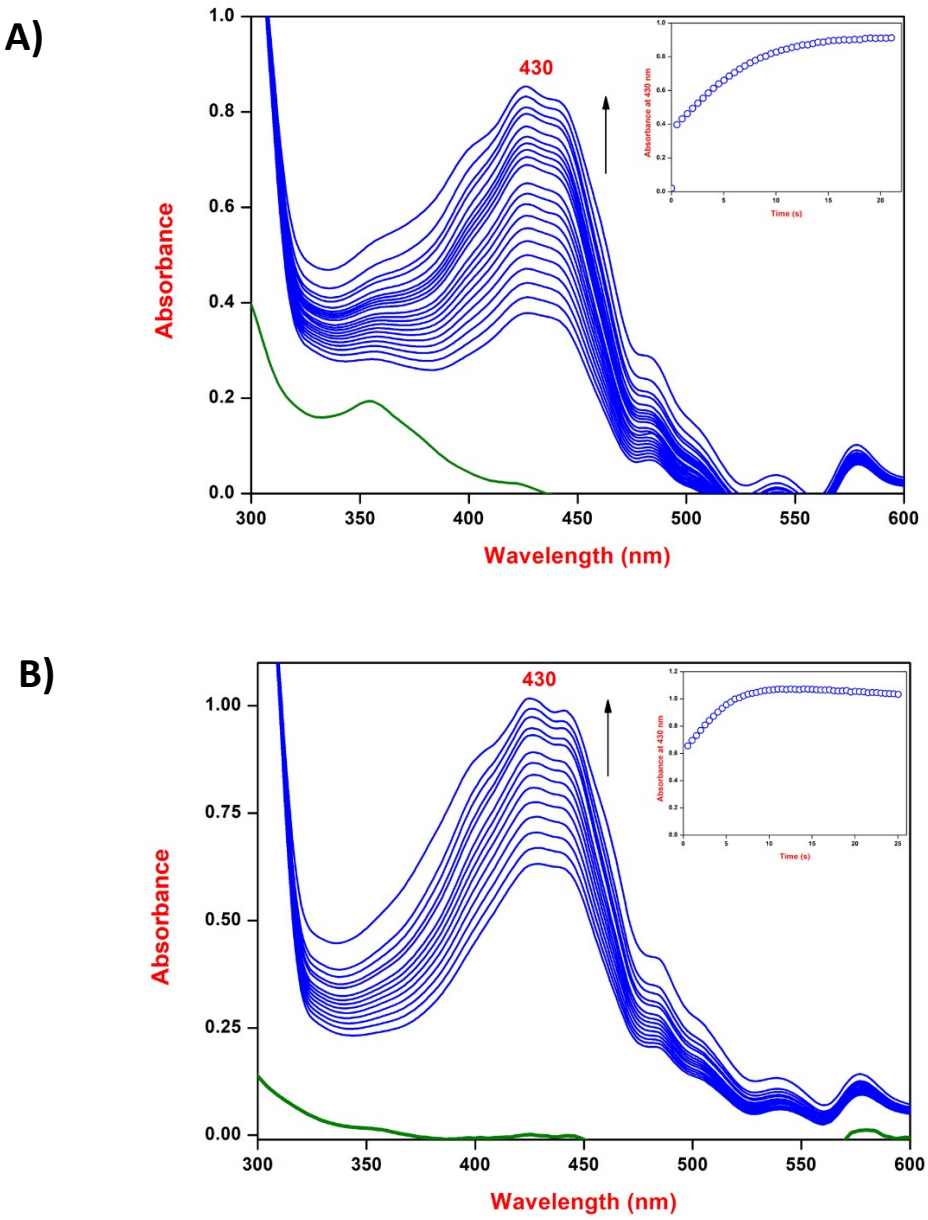

Figure S14. (A). UV-vis spectral changes showing the formation of phenoxazinone chromophore at 430 nm upon the addition of *o*-aminophenol (1.33×10^{-4} M) to a solution of **1** (A) and **3** (B) (3.33×10^{-6} M) in H_2O at room temperature in the presence of O_2. Inset shows the time trace of the reaction.

Figure S15

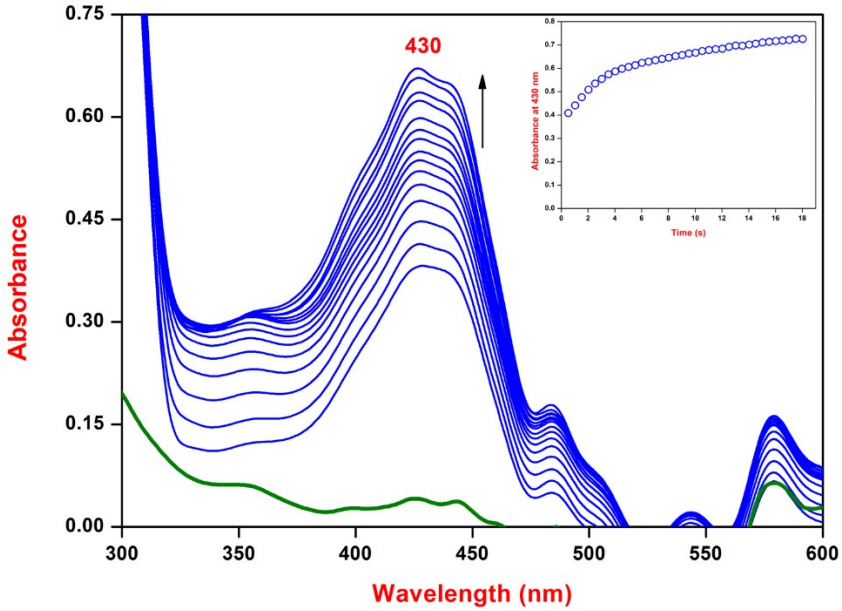

Figure S15. (A). UV-vis spectral changes showing the formation of phenoxazinone chromophore at 430 nm upon the addition of *o*-aminophenol (1.33×10^{-4} M) to a solution of **4** (3.33×10^{-6} M) in H_2O at room temperature in the presence of O_2. Inset shows the time trace of the reaction.

Figure S16

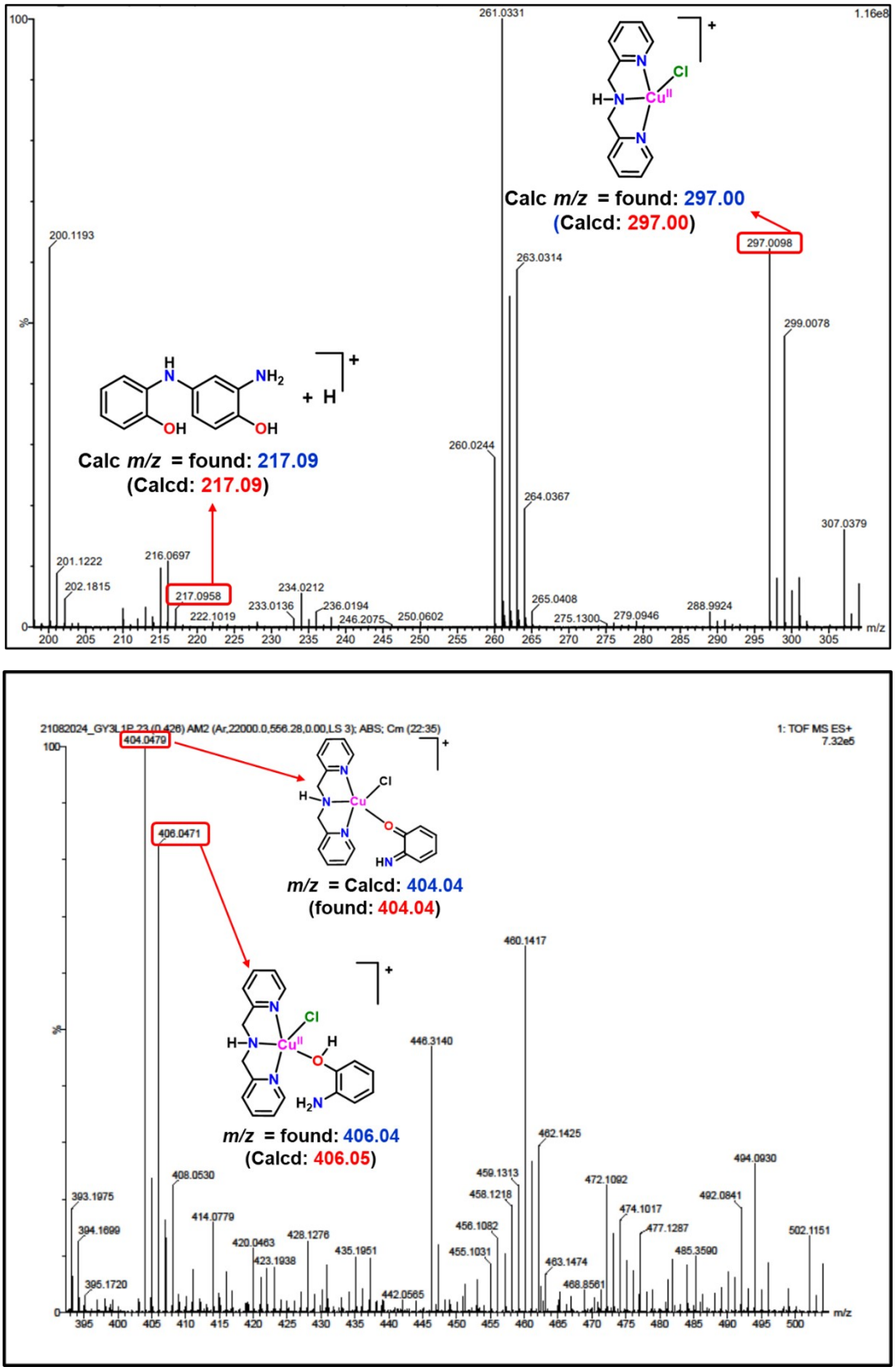

Figure S16. ESI-MS profile of 1:50 mixture of **1** and H_2AP in methanol-water (1:1 v/v) mixture.

Figure S17

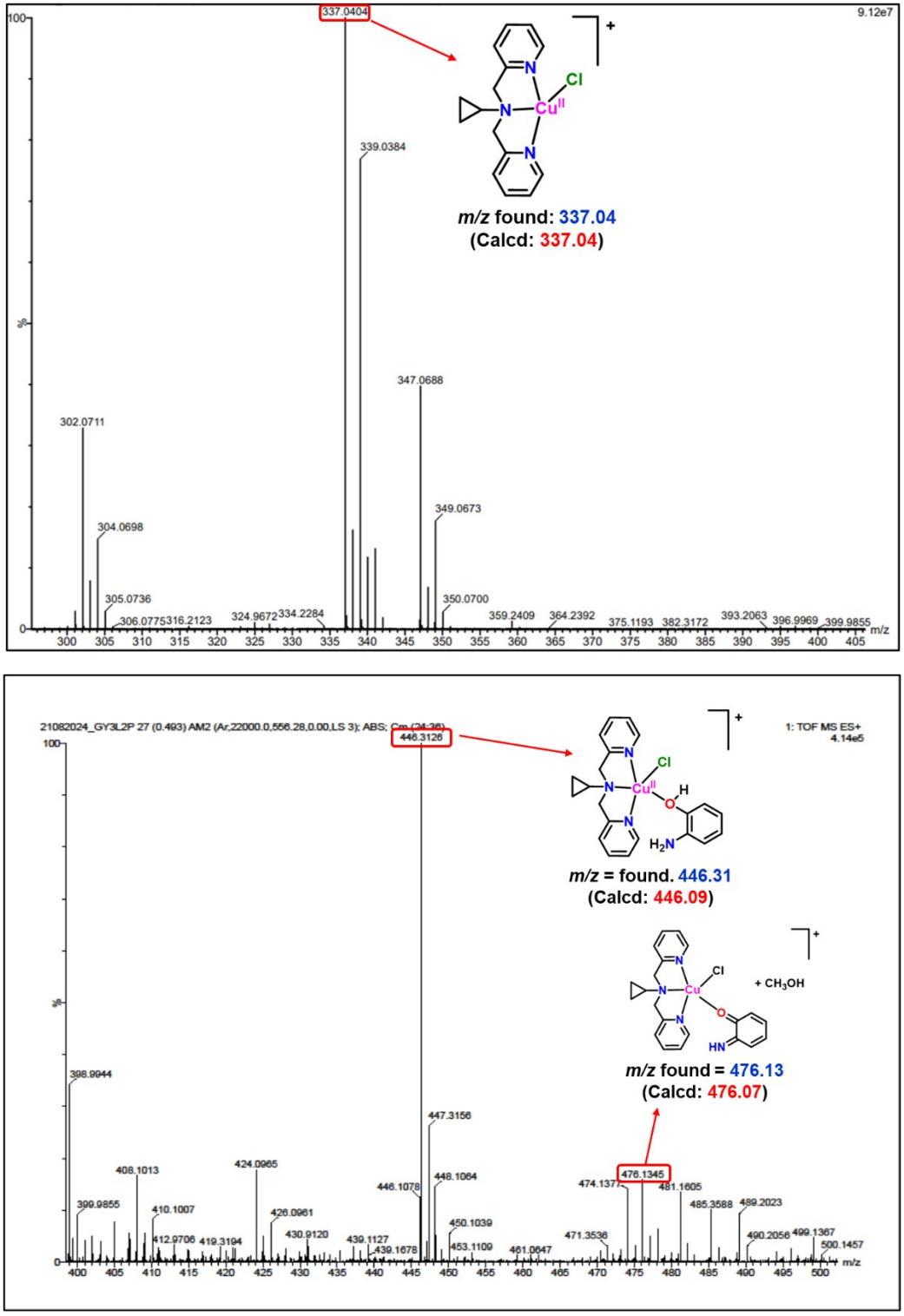

Figure S17. ESI-MS profile of 1:50 mixture of **2** and H_2AP in methanol-water (1:1 v/v) mixture.

Figure S18

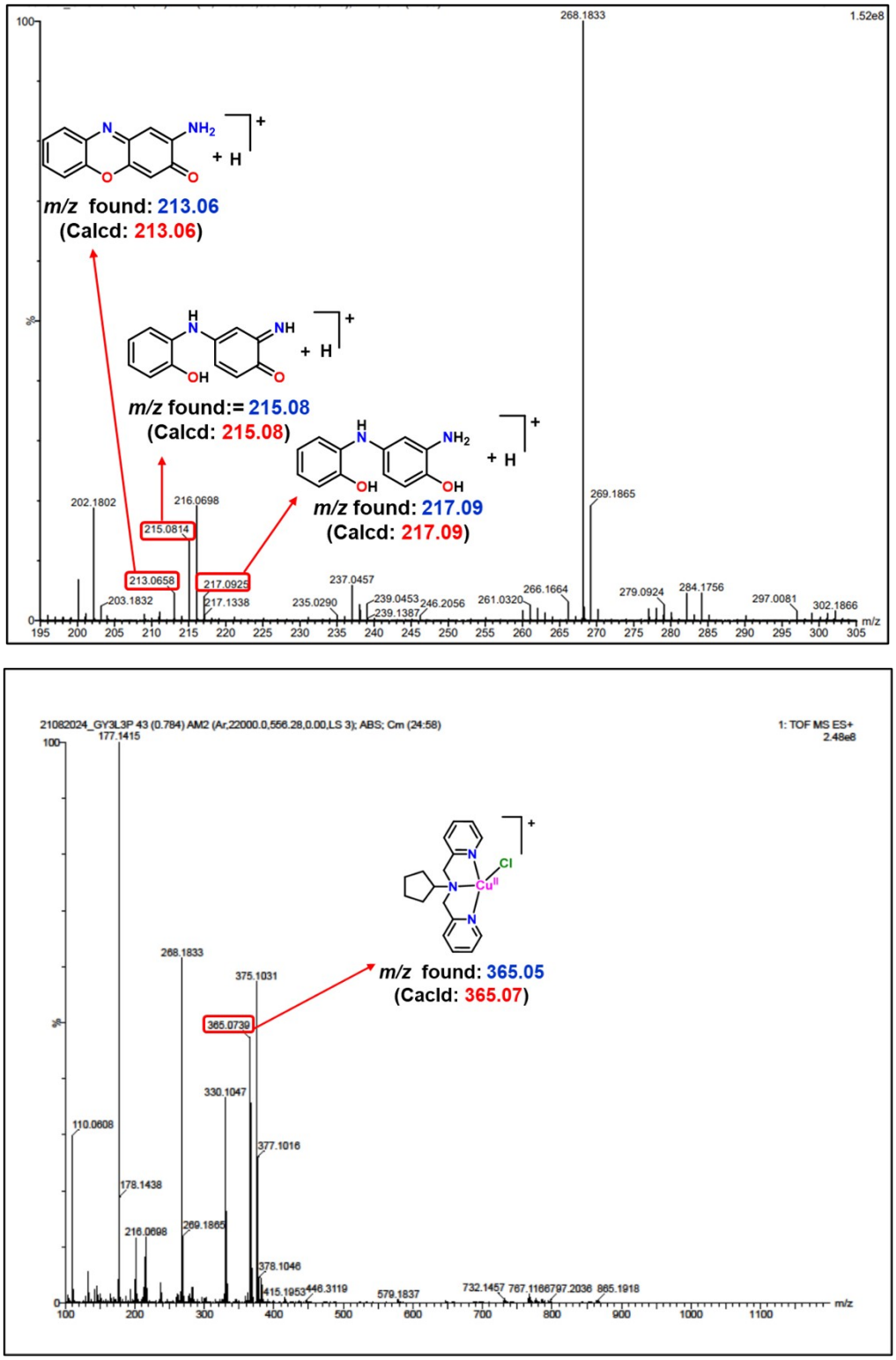

Figure S18. ESI-MS profile of 1:50 mixture of **3** and H_2AP in methanol-water (1:1 v/v) mixture.

Figure S18a

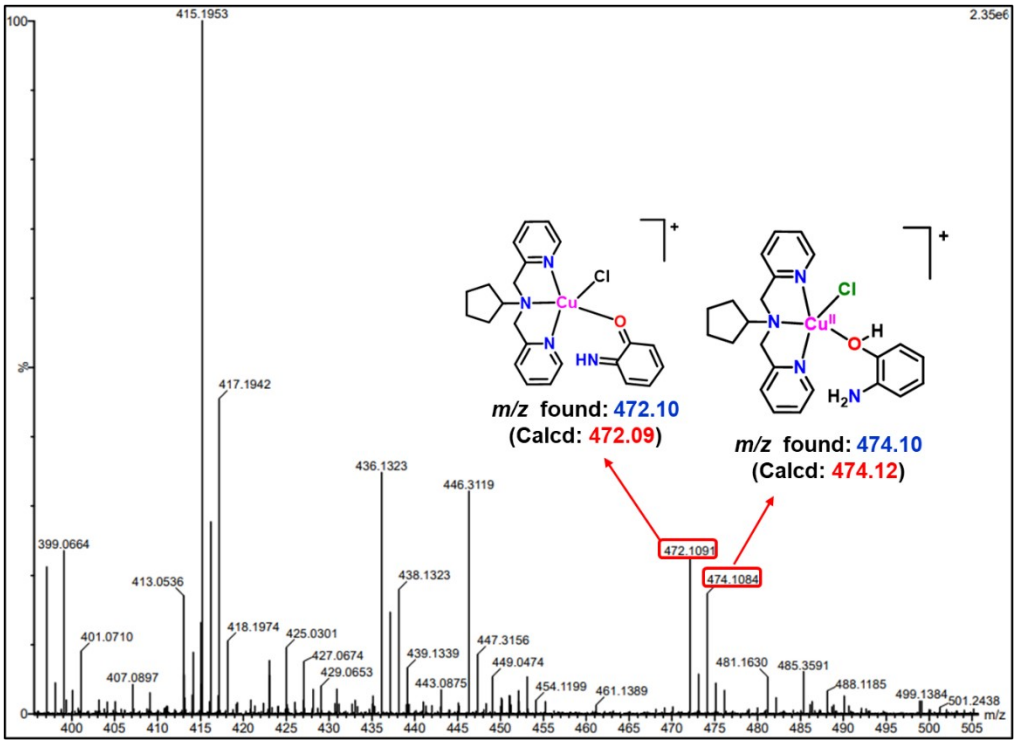

Figure S18a. ESI-MS profile of 1:50 mixture of **3** and H_2AP in methanol-water (1:1 v/v) mixture.

Figure S19

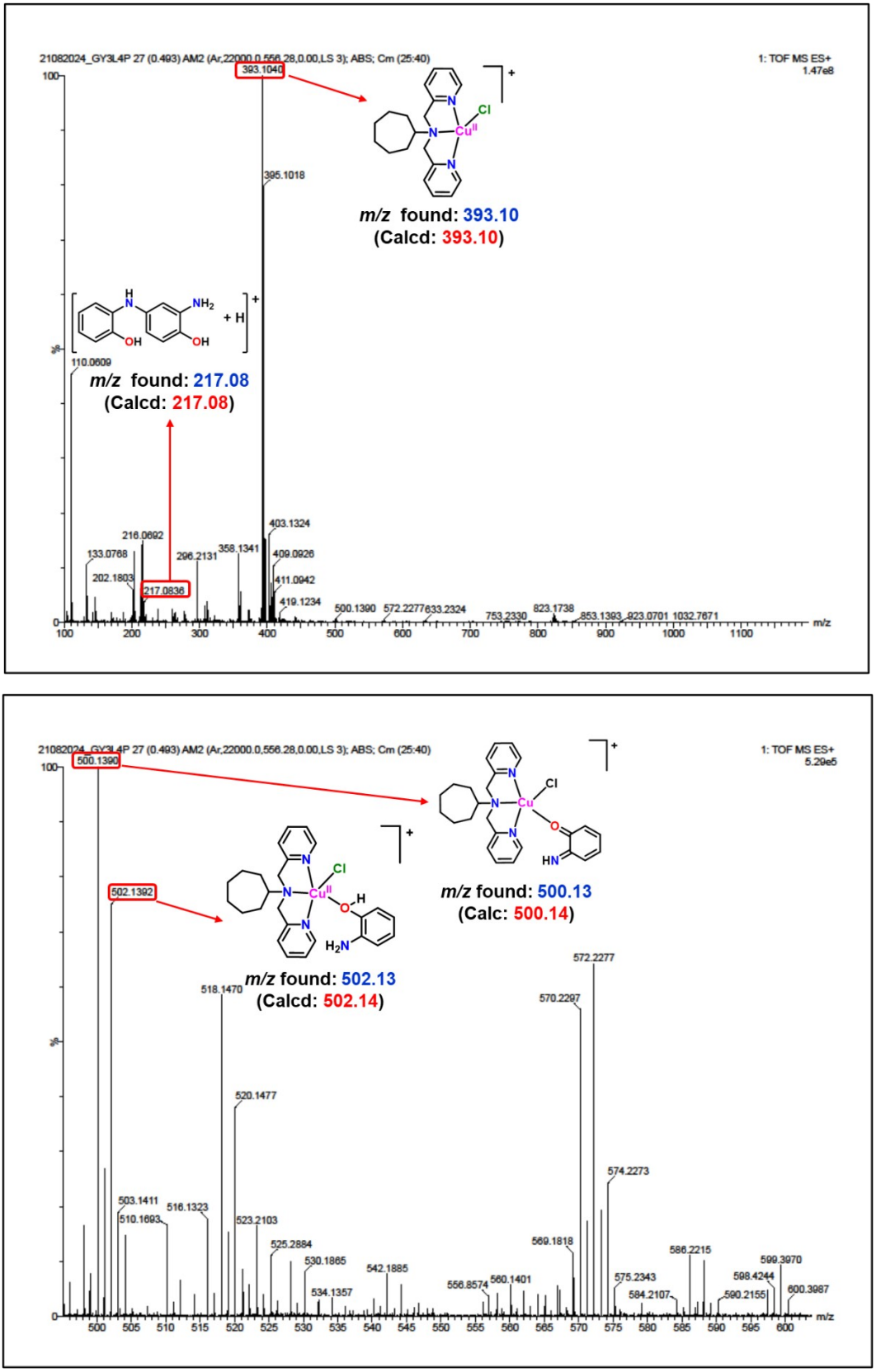

Figure S19. ESI-MS profile of 1:50 mixture of **4** and H_2AP in methanol-water (1:1 v/v) mixture.

Figure S20

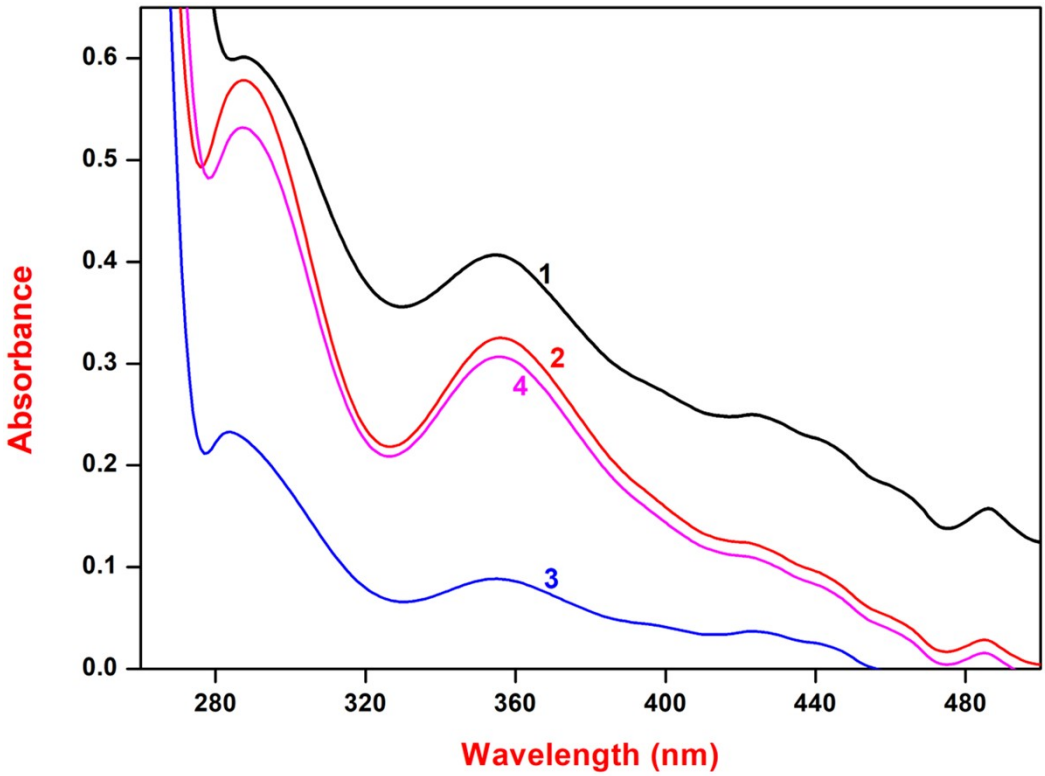

Figure S20. Detection of H_2O_2 by UV-vis spectroscopy during the oxidation of *o*-aminophenol catalysed by copper(II) complexes **1**–**4** in dioxygen saturated water solution.

Figure S21

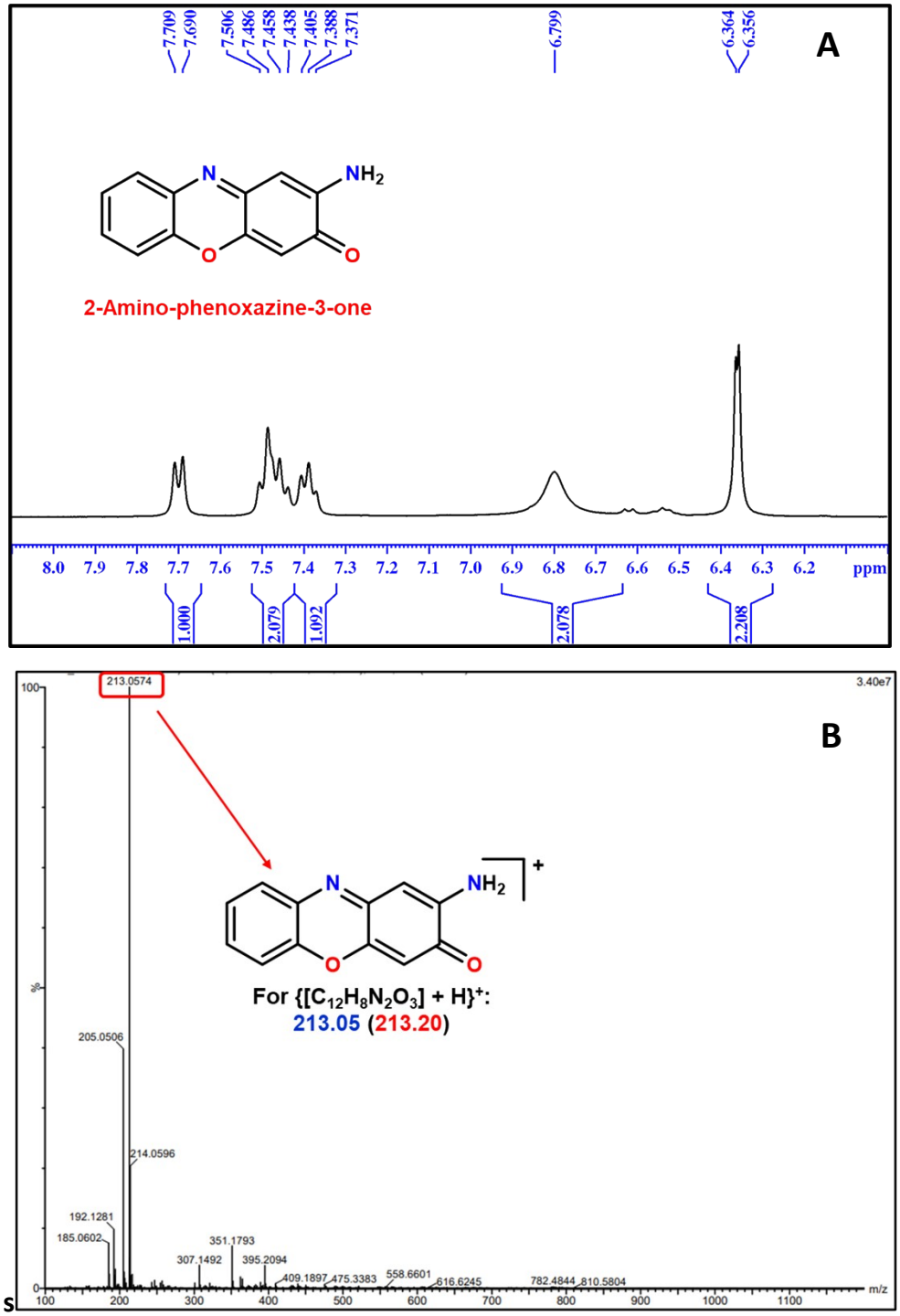

Figure S21. (A) ^{1}H NMR spectra of APX isolated from the kinetic solution and (B) ESI-MS profile of APX product.

Figure S22

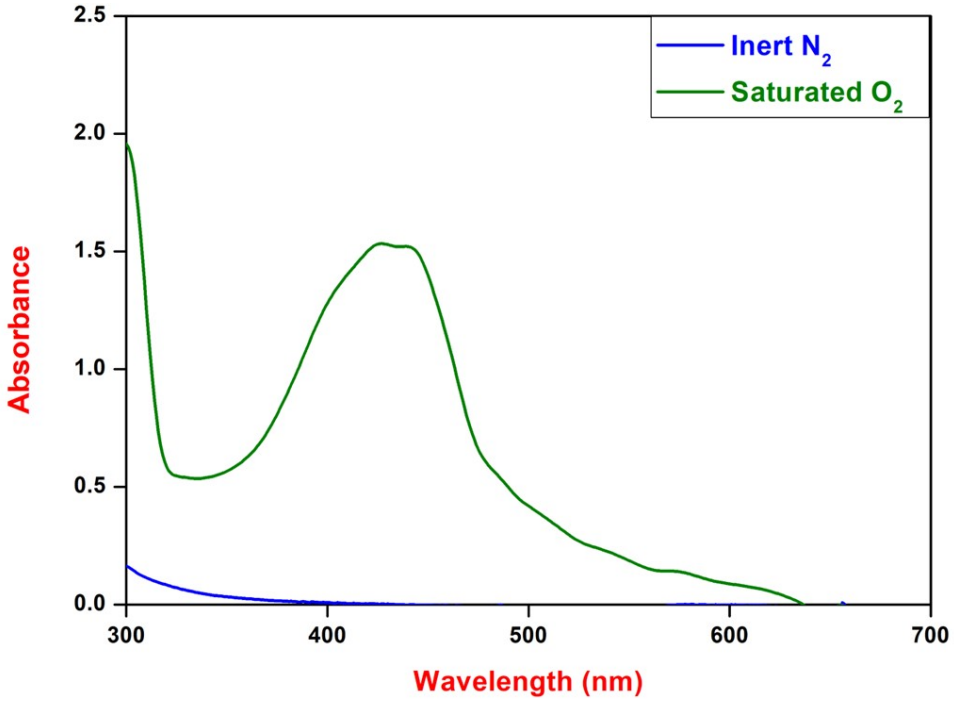

Figure S22. UV-vis spectral changes of copper(II) complex **2** with 50 equiv. of substrate under N_2 atmosphere (blue) and O_2 atmosphere (green) in aqueous medium.

Table S1. ATR-IR spectral data of ligands **L1**–**L4** and complexes **1**–**4**.

Stretching vibration (cm^{-1})	L1	1	L2	2	L3	3	L4	4
$\nu_{(O-H)}$	-	3531	-	3486		3419	-	3424
$\nu_{(N-H)}$	3380	3361	-	-	-	-	-	-
$\nu_{(C-H)}$	2960	2896	2950	2896	2955	2934	2931	2896
$\nu_{(C=N)}$	1595	1471	1595	1454	1585	1571	1446	1436
$\nu_{(M-N)}$	-	543	-	531	-	520	-	542

Table S2. TG-DSC data of copper(II) complexes **1–4**.

Complex	Temperature range (˚C)	Weight loss (%)	Assignments	ΔH (J g^{-1})
1	35–270	16		-285.76
	270–470	18.61	Decomposition of ligand moiety	-155.76
	470–600	47.19	Formation of CuO	-1591.40
2	35–260	23		-556.56
	260–340	25.29	Decomposition of ligand moiety	-884.73
	340–740	15.98	Formation of CuO	-2.72
3	35–215	5.5		-
	215–320	19.0	Decomposition of ligand moiety	-683.61
	320–575	54.5	Formation of CuO	-4377.13
4	35–220	11.32		-
	220–300	18.88	Decomposition of ligand moiety	-85.36
	300–515	45.23	Formation of CuO	-1937.77